First-principles investigation of chemical modification on two-dimensional iron–phthalocyanine sheet*

Wang Hong-Bo(王洪博), Su Yan(苏 燕)†, and Chen Gang(陈 刚)

Department of Physics, University of Jinan, Jinan 250022, *China*

(Received 8 May 2013; revised manuscript received 20 May 2013; published 2 December 2013)

Successful synthesis of single iron–phthalocyanie (FePc) framework layer on substrate and its transferrable properties open the door for decorating the separately distributed transition metals for exploring the diverse properties. We have studied the effects of chemical modification on two-dimensional FePc organometallic framework with density functional theory. For simplicity, the non-metal atoms with variant valence electrons are used as prototypes to estimate the effects from chemical modifications with different functional groups. The thermo-stabilities of the non-metal atom decorated complex sheet materials have been estimated by the first-principles constant energy molecular dynamic simulations. Upon the non-metal atom adsorption, the magnetic moment could be changed from 2 μ_B to 0, 1, 2, and 3 μ_B per unit cell for the case of tetra-, penta-, hexa-, and hepta-valent non-metal modifications, respectively, showing interesting promise to tailor its magnetic properties for potential applications.

Keywords: first-principles calculation, novel two-dimensional nanostructure, functional group decoration

PACS: 81.05.ue, 81.05.Rm, 81.05.Zx **DOI:** 10.1088/1674-1056/23/1/018103

1. Introduction

The observation of one atomic layer graphite material known as graphene has triggered explosive studies of two-dimensional (2D) materials.[1–4] The mostly studied materials are the graphene and the boron nitride sheet-based materials. Their properties have aroused extensive attention in both theory and experiment, which in fact can be tuned by introducing atoms, molecules, functional groups, or structural defects. For example, the band gap of graphene or boron nitride sheet can be continuously engineered by controlling the ratio of hydrogenation or fluidization.[5–9] The patterned regularly distributed pores in the graphene sheet itself as the so-called graphene nanomesh[10] or in the hydrogen layer of the hydrogenated graphene known as hydrogen vacancy cluster[11] can not only tailor the energy band gap of sheet material for potential usage such as effective field-effect transistors,[12] but also open the possibilities in hosting guest species such as functional groups in the pores to prevent segregation of the separately distributed particles with the purpose to keep their intrinsic properties.[13,14] In particular, the transition metal (TM) directed assembly of regularly organized networks owing to the separately incorporated metal could have various potential technological usages, including catalysis, gas storage, molecular electronics, molecular magnetism, sensor design, optics, molecular switches, and so on. However, no studies on synthesizing this kind of porous graphene-based sheet materials with metal regularly incorporated in the pores have been reported yet.

Recent progress in embedding iron atoms in the 2D phthalocyanine (Pc) sheet provides a novel pathway to achieve the long-standing dream of 2D atomic sheets with regularly and separately distributed TM atoms beyond the graphene sheet. Abel *et al.*[15] successfully synthesized the well-ordered Fe embedded 2D organometallic sheet FePc through a metal-directed surface reaction. Remarkably, the synthesis procedure demonstrated on a metal surface can be extended onto a thin insulating film showing the transferability to a real device. Due to the fundamental importance, the studies on the electronic properties of free standing TMPc (TM=Cr–Zn) sheet materials are required by the experimental advances, which is the first step in understanding these materials deposited on diverse substrates. In theory, with the purpose to facilitate the further development and the corresponding applications, Zhou and Sun preformed systematic investigations using the first-principles method on understanding the TMPc sheet materials by focusing on the magnetic properties.[16] Also, Li *et al.* have recently explored the structures and the electronic properties of various FePc nanoribbons and nanotubes.[17] The advances achieved in both experiment and theory show the promising diverse application usage of the TMPc 2D sheet materials. As to the TMPc materials, due to the fact that the naked transition metal could be attached by different functional groups such as the atomic hydrogen atom, it would thus be highly desirable to carry out a systematic study on the chemical functionalization of the novel TMPc frameworks, which however is still lacking. In this study, we would like to perform a detailed analysis of the non-metal atom adsorbed FePc organometallic sheet as an

*Project supported by the Research Fund of Taishan Scholar, China (Grant No. TSHW20101004), the Natural Science Foundation of Shandong Province, China (Grant No. ZR2010AM027), and the National Natural Science Foundation of China (Grant No. 11074100).

†Corresponding author. E-mail: ss_suy@ujn.edu.cn

© 2014 Chinese Physical Society and IOP Publishing Ltd

example to estimate the effects from the adsorptions of different functional groups by using the density functional theory.

2. Computational details

Our spin-polarized first-principles calculations are carried out with the density functional theory as implemented in the Vienna *ab initio* simulation package.[18] The projected augmented wave (PAW) method[19] with a plane-wave basis set is used. The exchange and correlation energy are described by the generalized gradient approximation with the Perdew, Burke, and Ernzerhof (PBE) parameterization.[20] Based on the geometrical structures optimized on the level of PBE-GGA, we have then re-optimized the structures and studied the electronic properties with the GGA+U method by including the effects from the onsite repulsion for the transition metal. In order to describe the strongly correlated systems properly, we used the GGA+U method with a correlation energy of 4 eV and an exchange energy of 1 eV for iron, which are well tested and used in previous studies.[16,17,21–25] The Monkhorst-Pack k-mesh of $5 \times 5 \times 1$ is used to integrate the electronic properties.[26] The optimized unit cell parameters for FePc are $a = b = 10.65$ Å which are in agreement with the previously calculated values ($a = b = 10.7$ Å)[16] and the experimental values ($a = b = 11.5 \pm 1$ Å).[15] Moreover, the sheet material is separated by a space of 15 Å along the z direction in order to avoid the interaction between the sheet and its periodic images. The wave function is expressed with the plane wave basis set and a cut-off energy of 400 eV is used. During the structure optimization, all the atoms are fully relaxed until the energy and force converge to 1×10^{-6} eV and 0.01 eV/Å, respectively.

3. Results and discussion

We have first studied the bare FePc sheet and provided the geometrical configuration and the density of states (DOS) in Fig. 1. The magnetic moment was calculated to be 2 μ_B per unit cell and the magnetic coupling was found to be antiferromagnetic (AFM). In fact, the antiferromagnetic state is almost degenerated in total energy with the ferromagnetic (FM) state. The AFM coupling is only around 2 meV than the FM one, indicating a quite weak coupling strength between the embedded Fe atoms. The weak coupling may be attributed the long interatomic distance of ~ 11 Å between two nearest Fe atoms. The facts of the weak magnetic coupling have been also found in our studies of the functionally modified FePc sheets. These properties make them to be interesting candidates for the metamagnetic materials. As reported previously, the AFM state of the metamagnetic materials could be switched to the FM state by an external field to induce the giant magnetoresistance.[27,28] The magnetic-field-induced transformation of the metamagnetic materials makes them to be interesting magnetic materials toward applications. The magnetic strength can be associated with the magnetic moment of each magnetic domain. Thus, in the latter of this paper, we would like to analyze the modification with the non-metal functionalization on the magnetic properties of each unit cell domain. As discussed in the section of introduction, the TMPc sheet materials could be fabricated on diverse device. As to the sides of the supported sheet materials, the chemical modification would probably happen on the naked side. Thus, the study on the chemical modification on one side of the free standing TMPc sheets would be desirable in view of its fundamental importance.

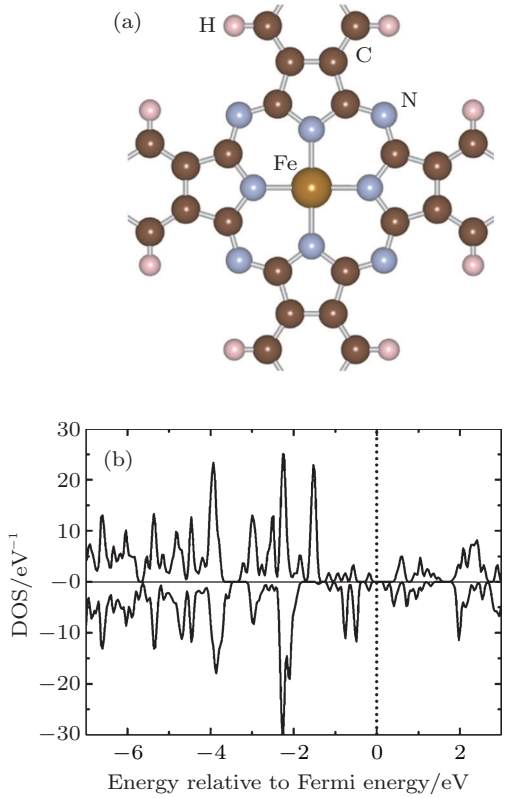


Fig. 1. (color online) Schematic configuration of (a) the FePc framework and (b) the densities of states of FePc, where the upward is for spin-up and the downward is for spin-down electrons.

In our studies, by putting single non-metal atoms (elements of groups IA and IIIA–VIIA) on the top of each iron, we have optimized the structures of *X*FePc (*X* stands for the non-metal element) and performed the constant energy first-principles molecular dynamics (MD) simulations. The MD simulation lasts for 5 ps with a time step of 1 fs. The temperature evolution as a function of simulation time for the C and F adsorbed FePc sheets are presented in Fig. 2, which are used as illustration for the temperature evolution of all the studied materials in this paper. The temperature is found at around 400 K. The structures obtained at the end of the simulations are found to have only slight distortions. Our simulations of all the other

studied non-metal atoms adsorbed FePc sheets show the similar results, suggesting their thermo-stabilities above the room temperature. We have also estimated the energies required to dissociate the XFePc complex sheet materials into the fragments of the XFe dimers and the two dimensional Pc sheet, which are calculated to be greater than 6 eV in our studies (see Table 1). For the chemisorption of non-metal atoms, we have calculated the binding energies as also listed in Table 1, which ranges from 0.62 eV for arsenic to 4.11 eV for carbon. Combining the study on the thermo-stability, the energy for fragmenting the complex material, and the binding energy for the non-metal atom chemisorption, we conclude that the single atom adsorbed material can gain its presence providing to introduce single atom source to the naked FePc sheet or *X*Fe dimers to the Pc sheet in experiment.

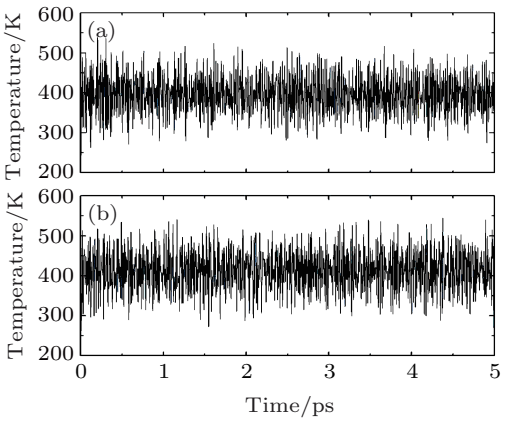


Fig. 2. Temperature evolution as a function of the simulation time of the constant energy for (a) CFePc and (b) FFePc.

In addition to H, the other studied non-metal atoms adsorption draws the iron out of the sheet plane by about 0.3 Å as presented in Table 1. The calculated bond lengths between the non-metal atoms and the iron are also presented in Table 1, which are found to be close to the corresponding interatomic distances of the free standing XFe dimers. Also, our charge density distribution studies clearly show charge accumulation between the adsorbates and the iron atom, confirming the chemical interaction.

For the non-metal atom adsorbed FePc sheet, we have also studied the electronic properties. We have presented the DOSs of the H, B, C, N, O, F chemisorbed FePc sheets in Fig. 3 and provided the corresponding HOMO–LUMO band gaps of the spin-up and spin-down electrons in the Table 1. The H atom less of empty p orbitals can only develop chemical bond pairing the H 1s electron with a Fe 3d electron, which is calculated to have 1.43 eV binding energy. Boron due to the $1s^2 2s^2 2p^1$ electronic configuration has a small negativity value. For the case of B chemisorption, the unpaired 2p electron could bond with a Fe 3d electron, the other unfilled 2p orbitals were found in our partial density of states study to locate above the Fermi level of the FePc sheet which hinders their hybridization with the occupied Fe 3d orbitals. The calculated magnetic moment per unit cell changes from 2 μ_B for the bare FePc sheet to 1 μ_B for the case of H and B modified FePc sheets. Compared to the DOS of bare FePc in Fig. 1, the DOSs shown in Fig. 3 for the C, O, N, and F adsorption are severely modified indicating stronger orbital hybridization. In our study of partial density of states, we have found that the 2s and 2p orbitals of carbon hybridize together showing an extensive overlapping of their densities of the states. The stronger bond between C and Fe has been developed. Due to both the sp

Table 1. The group of the element (the number of the valence electrons was provided in the brackets), the studied non-metal atom, the magnetic moment M per unit cell (in μ_B), the binding energy E_b (in eV) of the non-metal atom adsorption, the energy cost E_d (in eV) to dissociate the *X*FePc (*X* stands for non-metal atom) complex material to *X*Fe dimer and Pc fragments, the HOMO–LUMO band gaps for the spin-up (E_{g1}, in eV) and spin-down (E_{g2}, in eV) electrons respectively, the height increase h (in Å) of Fe out of the sheet plane induced by guest atom adsorption, the bond length D (in Å) of *X*Fe in *X*FePc sheet, and the bond length d (in Å) of the free standing XFe dimer.

Group	Element	M	E_b	E_d	E_{g1}	E_{g2}	h	D	d
IA (1)	H	1	1.43	7.83	0.43	0.15	0.06	1.47	1.46
IIIA (3)	B	1	2.35	8.20	0.45	0.50	0.23	1.72	1.76
IVA (4)	C	0	4.11	8.83	0.44	0.44	0.35	1.55	1.64
	Si	0	1.92	8.04	0.49	0.43	0.26	2.04	2.22
VA (5)	N	1	1.98	7.61	0.11	0.42	0.34	1.58	1.62
	P	1	0.90	7.21	0.30	0.43	0.29	2.02	2.10
	As	1	0.62	7.20	0.30	0.45	0.26	2.14	2.22
VIA (6)	O	2	3.52	7.08	0.39	0.37	0.27	1.64	1.63
	S	2	2.06	7.04	0.38	0.38	0.27	2.04	1.99
	Se	2	1.54	6.91	0.25	0.32	0.26	2.18	2.14
VIIA (7)	F	3	4.01	7.68	0.41	0.25	0.32	1.84	1.77
	Cl	3	2.56	7.51	0.45	0.20	0.31	2.24	2.11
	Br	3	2.04	7.49	0.40	0.22	0.30	2.40	2.24
	I	3	1.52	7.44	0.40	0.18	0.30	2.63	2.42

hybridization and the interaction between the carbon and the central iron, the densities of the states were extensively broadened agreeing with the strong C–Fe bonding as suggested by the binding energies presented in Table 1. As to the studied DOSs of spin-up and spin-down electrons shown in Figs. 1 and 3, their distribution was modified from the unsymmetrical distribution of bare FePc sheet to the symmetrical one of carbon chemisorbed sheet. The strong C–Fe bond strength combining the C sp hybridization effects may account for the magnetism diminishment. The unpaired 2p electrons are 3, 2, and 1 for the penta-, hexa-, and hepta-valence elements which could develop orbital hybridization with the Fe 3d oribitals. The binding energies per bond follow the sequence of penta- $<$ hexa- $<$ hepta-valence elements when compared in the same row of the periodic table. As presented in Fig. 3, the DOSs of the spin-up and spin-down orbitals still show unsymmetrical distribution for the N, O, and F adsorbed materials, showing their magnetic properties. In Table 1, we provided the calculated magnetic moments for the studied non-metal atoms adsorbed FePc sheets which are 0, 1, 2, and 3 μ_B per unit cell for the tetra-, penta-, hexa-, and hepta-valence atoms adsorbed FePc sheets, respectively. These results suggest an interesting pathway to tailor the magnetic properties of FePc sheet by functional group modification, which may also be a valid route to modify the magnetic properties of the other transition-metal phthalocyanine organometallic sheets toward potential application demand.

In Fig. 4, we have shown the magnetism distribution of the C, N, O, and F adsorbed FePc frameworks. For the H and B adsorbed FePc frameworks, the magnetism are found to distribute around the central Fe atom in our studies. The obvious Jahn–Teller distortion deviating from the C_{4v} point group symmetry occurs for the H and B decorated FePc. The guest atom adsorbed above the central Fe atom deviates away the symmetrical axis that is perpendicular to the sheet and goes across the Fe atom position. In the Figs. 3(a) and 3(b), we have also provided the densities of states of the H and B adsorbed FePc frameworks in the configurations without Jahn–Teller distortion. In comparison, the Jahn–Teller distortion splits the degenerated frontier bands around the Fermi level accordingly. The energy gain induced by the distortion is around 0.03 and 0.20 eV for the HFePc and BFePc, respectively. The HOMO–LUMO band gaps are enlarged from 0.44 eV and 0.06 eV to 0.46 eV and 0.17 eV of the spin-up and spin-down electrons of the HFePc. The effects from the Jahn–Teller distortion on the gaps of the BFePc are severe, which result in the 0.45 and 0.50 eV gaps for the spin-up and spin-down electrons in comparison with the 0.20 and 0 eV gaps of the C_{4v} structure. In our studies, no obvious Jahn–Teller distortion happens for the C, N, O, and F adsorption. Their band gaps are greater than 0.3 eV for both spin-up and spin-down electrons. As shown in Figs. 4(b)–4(d), the magnetism is dominatingly distributed around both the central iron and the adsorbates for the N, O, and F adsorbed FePc sheets.

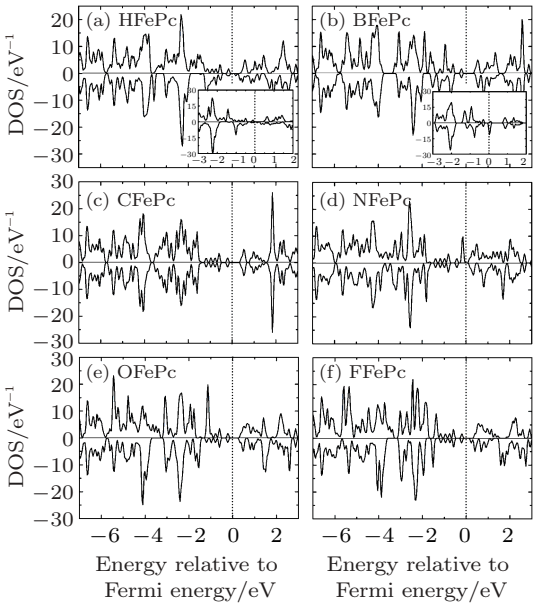


Fig. 3. The studied densities of states of (a) H, (b) B, (c) C, (d) N, (e) O, and (f) F modified FePc frameworks. The inserts in (a) and (b) are the corresponding densities of the H and B adsorbed FePc sheets in the configurations without Jahn-Teller distortion. The upward and the downward distribution are for the spin-up and the spin-down electrons, respectively.

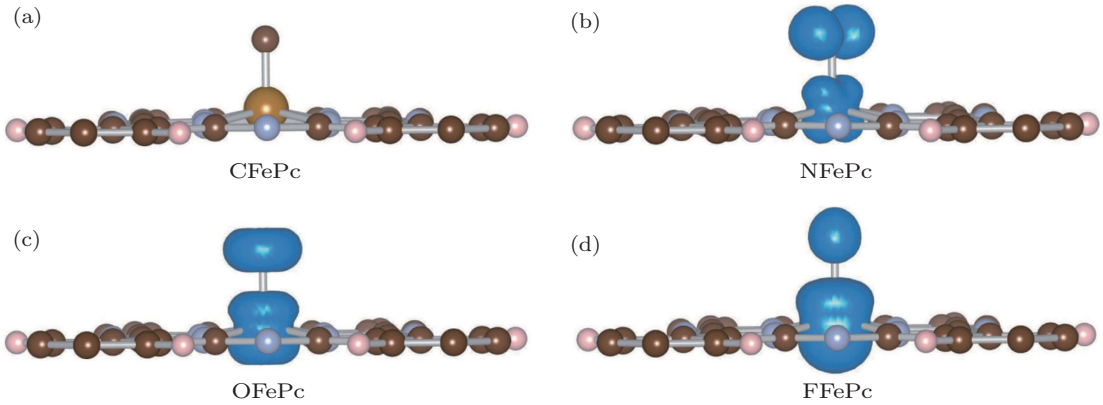


Fig. 4. (color online) Magnetism distribution at the iso-value of 0.01 μ_B/Å^3 for (a) C, (b) N, (c) O, and (d) F modified FePc frameworks.

4. Conclusions

The studied thermal stability, the binding energy, and the energy cost required to dissociate the complex material into fragments suggest the possibility in synthesizing the functional group modified FePc complex sheet materials. The H or B adsorption changes its magnetic moment to be 1 μ_B per unit cell. The obvious Jahn–Teller distortion occurs for the H and B adsorbed FePc frameworks. The magnetism of the FePc sheet could be tailored from 2 μ_B to 0, 1, 2, and 3 μ_B per unit cell for the case of the tetra-, penta-, hexa-, and hepta-valence atoms adsorption, respectively, showing the promise in engineering the magnetism of TMPc organometallic sheets by functional groups in different oxidation states either in a uniform one atomic layer or in a patterned configuration. This kind of materials could be expected to experience the magnetic-field-induced phase transformation from the AFM state to the FM state showing interesting potential applications.

References

[1] Novoselov K S, Geim A K, Morozov S V, Jiang D, Zhang Y, Dubonos S V, Grigorieva I V and Firsov A A 2004 *Science* **306** 666
[2] Novoselov K S, Geim A K, Morozov S V, Jiang D, Katsnelson M I, Grigorieva I V, Dubonos S V and Firsov A A 2005 *Nature* **438** 197
[3] Zhang Y, Tan Y W, Stormer H L and Kim P 2005 *Nature* **438** 201
[4] Zhang J, Zhang G Y and Shi D X 2013 *Chin. Phys. B* **22** 057701
[5] Sluiter M H F and Kawazoe Y 2003 *Phys. Rev. B* **68** 085410
[6] Elias D C, Nair R R, Mohiuddin T M G, Morozov S V, Blake P, Halsall M P, Ferrari A C, Boukhvalov D W, Katsnelson M I, Geim A K and Novoselov K S 2009 *Science* **323** 610
[7] Zhou J, Wang Q, Sun Q, Chen X S, Kawazoe Y and Jena P 2009 *Nano Lett.* **9** 3867
[8] Chen W, Li Y, Yu G, Li C Z, Zhang S B, Zhou Z and Chen Z 2010 *J. Am. Chem. Soc.* **132** 1699
[9] Lu D, Yang Y R, Xiao Y and Zhang X Y 2011 *Chin. Phys. B* **20** 118101
[10] Bai J, Zhong X, Jiang S, Huang Y and Duan X 2010 *Nat. Nanotechnol.* **5** 190
[11] Singh A K, Penev E S and Yakbson B I 2010 *ACS Nano* **4** 3510
[12] Lin X, Wang H L, Pan H and Xu H Z 2011 *Chin. Phys. B* **20** 047302
[13] Dai X Q, Tang Y N, Dai Y W, Li Y H, Zhao J H, Zhao B and Yang X 2011 *Chin. Phys. B* **20** 056801
[14] Li Q X, Yang J L, Yuan L F, Hou J G and Zhu Q S 2001 *Chin. Phys. Lett.* **18** 1234
[15] Abel M, Clair S, Ourdjini O, Mossoyan M and Porte L 2011 *J. Am. Chem. Soc.* **133** 1203
[16] Zhou J and Sun Q 2011 *J. Am. Chem. Soc.* **133** 15113
[17] Li L H, Li J Q and Wu L M 2012 *J. Phys. Chem. C* **116** 9235
[18] Kress G and Furthmüller J 1996 *Phys. Rev. B* **54** 11169
[19] Kress G and Joubert D 1999 *Phys. Rev. B* **59** 1758
[20] Perdew J P, Burke K and Ernzerhof M 1996 *Phys. Rev. Lett.* **77** 3865
[21] Okabayashi J, Kimura A, Rader O, Mizokawa T, Fujimori A, Hayashi T and Tanaka M 1998 *Phys. Rev. B* **58** R4211
[22] Sato K, Bergqvist L, Kudrnovský J, Dederichs P H, Eriksson O, Turek I, Sanyal B, Bouzerar G, Katayama-Yoshida H, Dinh V A, Fukushima T, Kizaki H and Zeller R 2010 *Rev. Mod. Phys.* **82** 1633
[23] Sato K, Dederichs P H, Katayama-Yoshida H and Kudrnovský J 2004 *J. Phys.: Condens. Matter.* **16** 5491
[24] Bernien M, Miguel J, Weis C, Ali Md E, Kurde J, Krumme B, Panchmatia P M, Sanyal B, Piantek M, Srivastava P, Baberschke K, Oppeneer P M, Eriksson O, Kuch W and Wende H 2009 *Phys. Rev. Lett.* **102** 047202
[25] Shick A B, Kudrnovsky J and Drchal V 2004 *Phys. Rev. B* **69** 125207
[26] Monkhorst H J and Pack J D 1976 *Phys. Rev. B* **13** 5188
[27] Zheng L M, Gao S, Song H H, Decurtins S, Jacobson A J and Xin X Q 2002 *Chem. Mater.* **14** 3143
[28] Zhang Y Q and Zhang Z D 2003 *Phys. Rev. B* **67** 132405